flow capacity due to the loss of sympathetic nerve-mediated graft vasoconstriction.

Materials and methods

Animal preparation

Animal care was provided in accordance with the *Guiding Principles for the Care and Use of Animals in the Field of Physiological Sciences* approved by the Physiological Society of Japan. All protocols were approved by the Animal Subject Committee of the National Cerebral and Cardiovascular Center. Five adult mongrel dogs (weighing 24–35 kg) were anesthetized with intravenous pentobarbital sodium (25 mg/kg) and intubated endotracheally for artificial ventilation with isoflurane and 100% O_2. After a median sternotomy, the heart was suspended in a pericardial cradle. To measure systemic arterial pressure, we placed a fluid-filled catheter in the left subclavian artery via the left brachial artery and connected it to a pressure transducer (DX-200; Nihon Kohden, Tokyo, Japan). The junction of the inferior vena cava and the right atrium was taken as the reference point for zero pressure. An ultrasonic flowmeter (20A594; Transonic Systems, Itaca, NY) was placed around the ascending aorta to measure cardiac output. Electrocardiography leads were also placed for the monitoring electrocardiogram. A catheter was inserted into the femoral vein for fluid replacement (1 ml/kg/h of Ringer's solution). All protocols were performed under open chest conditions.

Pedicled ITA grafting

The left internal thoracic artery (LITA), together with the surrounding veins, muscle, and fascia, was harvested as a pedicled graft using electrocautery. The LITA was harvested from the bifurcation of the musculo-phrenic and superior epigastric arteries up to the upper margin of the first rib or higher. All intercostal branches of the LITA were ligated. After systemic heparinization, the LITA was clamped, and the distal end of the LITA was cut and anastomosed to the left anterior descending artery (LAD). The same surgeon (D.U.) performed the LITA–LAD anastomosis without cardiopulmonary bypass. The heart and the LAD were stabilized using a compression-type mechanical stabilizer (Mini-CABG system; United States Surgical Corporation, Norwalk, CT). A shunt tube was inserted into the LAD to prevent myocardial ischemia during anastomosis. The anastomosis was placed in the mid-LAD [8]. The anastomosis was created using a continuous 7-0 polypropylene suture. The proximal LAD was first ligated after the LITA–LAD anastomosis, and then the LITA was declamped. An angiography was performed after the anastomosis to confirm the absence of stenosis or spasm in the LITA–LAD anastomosis. The LITA graft was sprayed with dilute papaverine (4 mg/ml) to prevent spasm. An ultrasonic flowmeter (2.5S261; Transonic Systems) was placed around the LITA just proximal to the anastomosis. The left stellate ganglion was carefully exposed through a median sternotomy, and a pair of platinum electrodes was attached to it without decentralization. The nerve and electrodes were covered with a mixture of silicone gel (Kwik-Sil; World Precision Instrument, Sarasota, FL). Protocol 1, described below, was carried out following the pedicled LITA grafting.

Skeletonized ITA grafting

Following the completion of protocol 1, the tissue surrounding the graft (including fascia and lymphatics) was stripped up to the most proximal part of the LITA graft in order to skeletonize the LITA graft. The side branches of the LITA were ligated. Fat tissue around the graft was removed as completely as possible based on macroscopic inspection. The adventitia was left as the outermost layer of the graft. The graft was not touched directly with forceps. The graft was sprayed with dilute papaverine (4 mg/ml). After skeletonizing the LITA graft, protocol 2 followed.

Experimental protocols

Since skeletonization always followed pedicled harvesting, protocol 1 (pedicled LITA graft flow measurement) was performed before protocol 2 (skeletonized LITA graft flow measurement) in all dogs. The stimulation of the left sympathetic stellate ganglion for adjusting the voltage amplitude was performed at least 30 min before protocol 1 was initiated.

Protocol 1

The left sympathetic stellate ganglion was electrically stimulated at least 30 min after the completion of the experimental preparation of the pedicled LITA grafts. The frequency of stimulation was increased stepwise from 0 to 10 Hz with increments of 2 Hz. Each step was maintained for 60 s. The pulse duration of the stimulus was set at 5 ms. The voltage amplitude of stimulation (2–5 V) was adjusted in each animal to yield an increase in arterial pressure of approximately 30 mmHg with 10 Hz stimulation. Graft flow, arterial pressure, and cardiac output were recorded for 7 min, which included a 2-min baseline and 5 min of stimulation. These data were sampled at 200 Hz using a 12-bit analog-to-digital converter [AD12-16U(PCI)E;

CONTEC, Osaka, Japan] and stored on the hard disk of a dedicated laboratory computer system.

Protocol 2

At least 30 min after the completion of the experimental preparation of the skeletonized LITA grafts, the left sympathetic stellate ganglion was electrically stimulated in a similar fashion to protocol 1, while all variables were recorded and stored.

Data analysis

Heart rate was calculated from the arterial pressure waveform. Myocardial oxygen demand was estimated as double product (pressure–rate product) and calculated as the product of systolic arterial pressure and heart rate [9]. All variables were averaged during the last 20 s of each electrical stimulation level.

Statistical analysis

All data are presented as the mean ± standard error (SE). In each protocol, one-way repeated measures analysis of variance (ANOVA) followed by Dunnett's test was used to compare variables at each stimulation against the baseline value. The paired t test was used to compare variables between pedicled and skeletonized LITA grafts at each stimulation level. Linear regression analysis was used to examine the relationship between the double product and graft flow. Differences were considered to be significant at a threshold of $P < 0.05$.

Results

Prior to sympathetic stimulation, baseline graft flow (under spontaneous sympathetic outflow) was greater in skeletonized ITA than pedicled ITA (Table 1). Other hemodynamic parameters, including heart rate, cardiac output, mean arterial pressure, and double product, did not differ significantly regardless of harvesting technique.

Table 1 Hemodynamic parameters and graft flow before stimulation

Hemodynamic parameters	Pedicled	Skeletonized	P value
Heart rate (beats/min)	104 ± 8	106 ± 8	NS
Mean arterial pressure (mmHg)	94 ± 7	93 ± 7	NS
Cardiac output (ml/min/kg)	83 ± 17	74 ± 9	NS
Double product (mmHg beats/min)	11368 ± 834	11346 ± 621	NS
Graft flow before stimulation (ml/min)	22.6 ± 2.7	27.8 ± 1.9	<0.05

Values are given as the mean ± standard error (SE)

NS Not significant

Graft flow patterns at baseline and under sympathetic stimulation are shown in Fig. 1a. Sympathetic stimulation increased graft flow ($P < 0.05$) similarly in skeletonized and pedicled ITA grafts, and maximal flow was comparable to each other at 10-Hz stimulation [nonsignificant (NS) difference] (Fig. 1b). Increases in systemic arterial pressure and heart rate did not differ significantly between the two techniques (Fig. 2), and increases in myocardial oxygen demand in response to sympathetic stimulation, as estimated by double product, were likewise similar.

Graft flow (y) correlated well with the double product (x) in both pedicled ($y = 2.6 \times 10^{-3}x - 8.4$, $R^2 = 0.73$) and skeletonized ITA ($y = 2.3 \times 10^{-3}x - 0.7$, $R^2 = 0.69$). The slope and y-intercept did not differ statistically between the two techniques (Fig. 3).

Discussion

The choice of either skeletonized or pedicled ITA grafts for CABG may be an important decision from both the technical and clinical viewpoints; however, clear evidence demonstrating the advantage of either method over the other is not yet available. In this study, we have shown that graft flow increased to a similar level during maximal sympathetic stimulation in both pedicled and skeletonized ITA grafts. These results do not support our hypothesis that the skeletonized ITA would provide larger flow capacity and indicate that coronary vasodilatation in response to increased myocardial oxygen demand is a stronger determinant of graft flow than any possible increase in the vascular resistance of ITA itself. Our study also demonstrates that both skeletonized and pedicled ITAs were able to supply adequate graft flow after CABG even during intense sympathoexcitation.

There are several possible explanations for the difference in graft flow under baseline conditions. First, a loss of sympathetic innervation in the skeletonized graft may have dilated the ITA relative to the pedicled graft under baseline conditions. In support of this explanation, Takami et al. [7] reported that the diameter of the ITA just proximal to the anastomosis is significantly larger in the skeletonized ITA than that in the pedicled ITA. Dönmez et al. [10] reported that the diameter of ITA becomes statically larger by the stellate ganglion blockade. In a preliminary study, we observed that electrical stimulation of the stellate ganglion decreased ITA flow before harvest. Therefore, vasoconstriction may occur in the pedicled ITA during sympathetic stimulation. However, in this study we did not perform simultaneous measurements of the graft flow and diameter

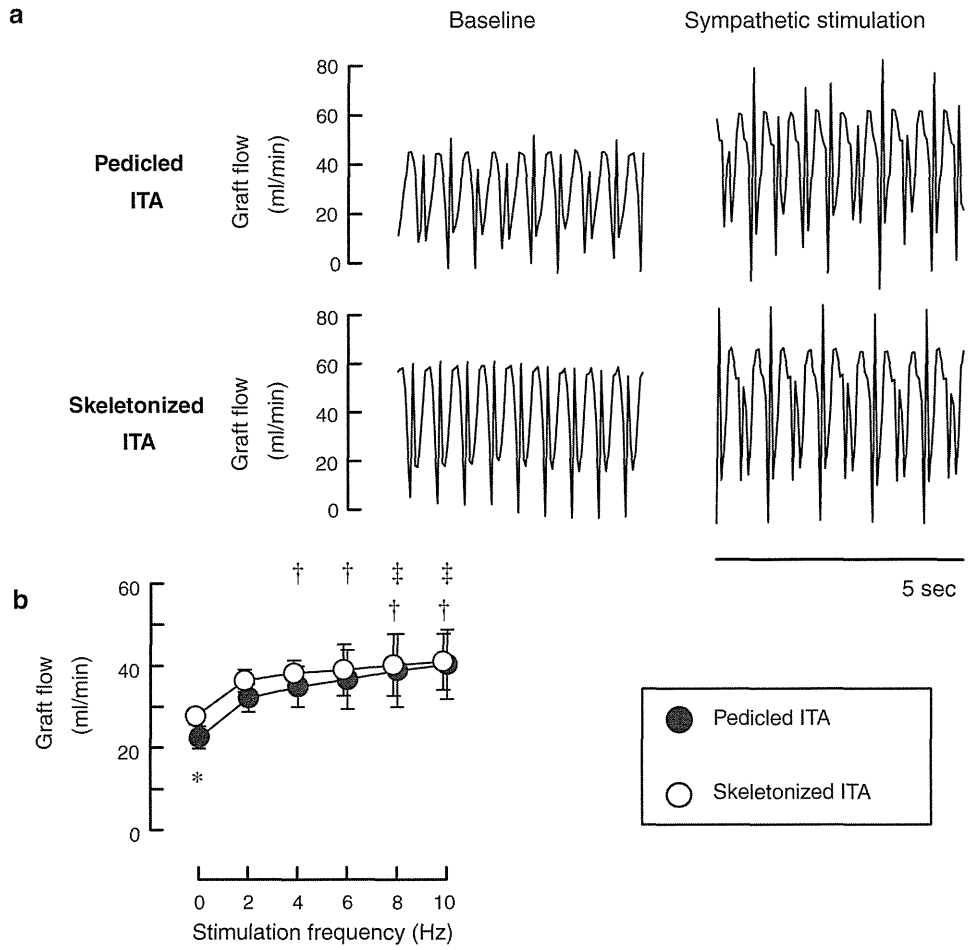

Fig. 1 **a** Typical representative recording of graft flow with pedicled and skeletonized internal thoracic arteries (*ITAs*) during sympathetic nerve stimulation. **b** Mean graft flow with pedicled (*closed circle*) and skeletonized (*open circle*) ITAs during sympathetic nerve stimulation. Data are shown as the mean ± standard error (SE). $^{\dagger}P < 0.05$ vs. baseline, $^{\ddagger}P < 0.01$ vs. baseline, $^{*}P < 0.05$ pedicled vs. skeletonized

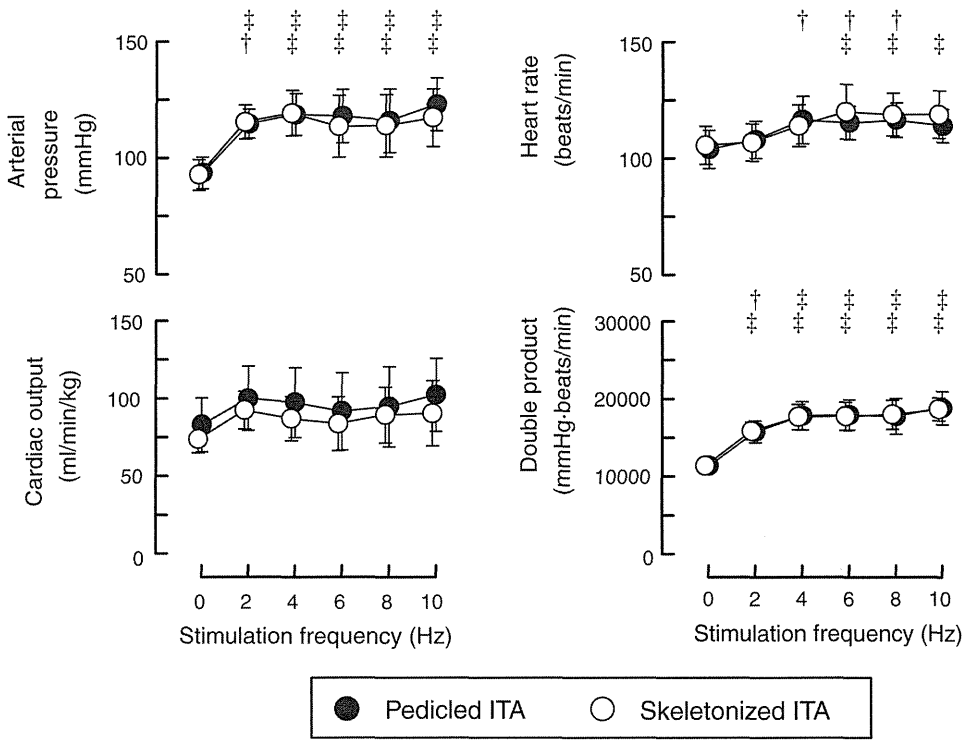

Fig. 2 Changes in mean arterial pressure, cardiac output, heart rate, and double product with pedicled (*closed circle*) and skeletonized (*open circle*) ITAs during sympathetic nerve stimulation. Data are shown as the mean ± SE. $^{\dagger}P < 0.05$ vs. baseline, $^{\ddagger}P < 0.01$ vs. baseline

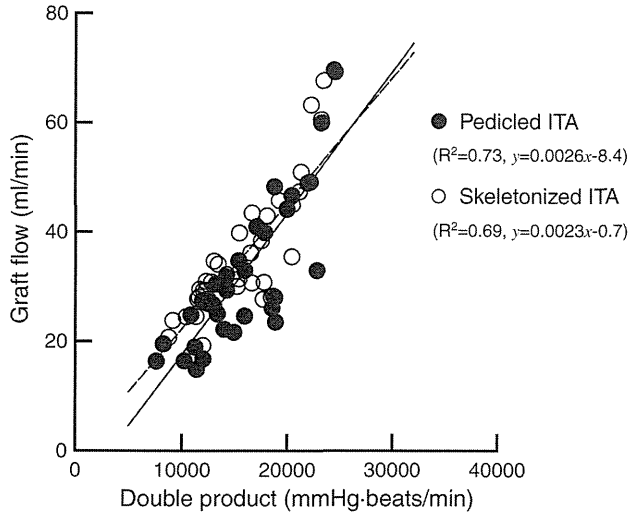

Fig. 3 Scatter plots and regressions between the double product and graft flow with pedicled (*closed circle*, *solid line*) and skeletonized (*open circle*, *dashed line*) ITAs. Regression lines did not differ between the two groups. y Graft flow, x double product

because the use of contrast medium in angiography may have affected the graft flow through its vasodilatative effect on the coronary artery [11].

Another explanation may be the difference in background sympathetic tone. As the skeletonized graft flow was always studied in the later phase of the experiment, when background sympathetic tone and myocardial metabolic demand may be higher, skeletonized graft flow may have been higher for this reason. The presence of similar hemodynamics during the two protocols, however, does not directly support this explanation. The hemodilution seen predominantly in the later phase of the experiment may also have contributed to higher flow through the skeletonized graft under baseline conditions.

The fact that graft flows were similar between the skeletonized and pedicled ITAs during maximal sympathetic excitation indicates that the resistance of the ITA graft was much smaller than that of the native coronary bed, even when the coronary bed was maximally dilated to meet the oxygen demand present with maximal sympathetic stimulation. In other words, both the skeletonized and pedicled ITAs would appear to provide sufficient flow reserve to the LAD area. In contrast, it has been reported that free flow, which may represent the maximal flow capacity of the ITA itself, is greater in the skeletonized ITA than in the pedicled ITA [2, 3]. Despite these previous findings, because the maximally dilated native coronary bed would be the most practical downstream conduit to test the difference between the skeletonized and pedicled ITAs, we believe that the difference in sympathetic innervation does not affect the maximal flow significantly under anastomosed conditions.

In addition to the effects of downstream resistance, local mechanisms would also contribute to the observed difference in flow between the pedicled and skeletonized ITA grafts. Complete sympathetic denervation with the local application of phenol to the skeletonized ITA further increased graft flow (unpublished observation), suggesting that there remains a certain sympathetic innervation in the skeletonized ITA. Even though sympathetic denervation may not be complete after skeletonization, we believe that our skeletonization did not differ greatly from those clinically performed by surgeons. Deja et al. [4] reported that skeletonization increases the reactivity of ITA to norepinephrine in vitro. Their study may support our results. Prior to sympathetic stimulation but under spontaneous sympathetic outflow, the amount of endogenous norepinephrine release to the skeletonized ITA may be relatively smaller than that to the pedicled ITA; as such, the sympathetic vasoconstriction would be negligible in the skeletonized ITA. This may explain the larger graft flow in the skeletonized ITA prior to sympathetic stimulation. Under maximal sympathetic stimulation, however, hyperreactivity to endogenous norepinephrine in the skeletonized ITA may cause the sympathetic vasoconstriction similar to that occurring in the pedicled ITA. This local mechanism may also partly account for why graft flow was comparable between the pedicled and skeletonized ITAs during maximal sympathetic stimulation. Although the results from several pharmacological studies suggest that norepinephrine-induced vasoconstriction does occur in the ITA [12, 13], there have been no reports assessing the tissue norepinephrine concentration of ITA during sympathetic stimulation. Further investigations are necessary to gain an understanding of the difference in norepinephrine reactivity between the pedicled and skeletonized ITAs.

Some publications have reported several advantages of the skeletonized ITA grafts other than the potential increase in graft flow at rest [1, 14]. Firstly, skeletonization lengthens the ITA, thereby providing access to more distal targets in the coronary artery [15]. Second, skeletonization improves blood supply to the sternum (measured by single photon emission computed tomography) [16] compared with pedicled harvesting. Third, skeletonization decreases the incidence of postoperative respiratory dysfunction because of less invasive harvesting (i.e., preserved pleural integrity in skeletonized ITA vs. pleurotomy in pedicled ITA) [17, 18]. Lastly, skeletonization markedly reduces anterior chest pain and dysesthesia 3 months after surgery [19]. In contrast to these advantages, skeletonization has the minor disadvantages of greater technical difficulty, longer harvesting duration, and potential damage to the graft.

Limitations

This study has several limitations. First, because skeletonized graft flow measurements always follow pedicled graft flow measurements in the same dog, the effect of time sequence on graft flows cannot be ruled out. Nevertheless, the similar hemodynamic response to sympathetic stimulation between protocol 1 and 2 (Fig. 2) suggests that the animal conditions did not deteriorate considerably. Second, the perfusion area of LITA was limited to the LAD region. If we had used a much larger perfusion area of LITA, the possible small difference between the pedicled and skeletonized ITAs may have been revealed. Third, a histological comparison between the pedicled and skeletonized ITA was not performed because the pedicled ITA was always skeletonized after the protocol 1, and the tissue samples from the pedicled ITA could not be obtained. Further investigations that include histological comparison are necessary for examining the effect of skeletonization on sympathetic innervations.

Conclusion

Both the pedicled and skeletonized ITA techniques supplied similar, adequate blood flow to the LAD, meeting myocardial oxygen demand during sympathetic excitation. Metabolic demand can override the possible difference in sympathetic vasoconstriction, increasing the flow in both pedicled and skeletonized ITA grafts to a similar extent when they are anastomosed to LAD. The results of this study have an important implication in terms of clinical application. Following anastomosis, graft flow is highly variable and is dependent on myocardial oxygen demand. Because the quality of CABG may be judged based on flow through anastomosed grafts, one has to take into consideration the potential change in flow in response to myocardial oxygen demand.

Acknowledgments This study was supported by Health and Labor Sciences Research Grants (H18-nano-Ippan-003, H19-nano-Ippan-009, H20-katsudo-Shitei-007 and H21-nano-Ippan-005) from the Ministry of Health, Labor and Welfare of Japan, by Grants-in-Aid for Scientific Research (No. 20390462) from the Ministry of Education, Culture, Sports, Science and Technology in Japan and by the Industrial Technology Research Grant Program from New Energy and Industrial Technology Development Organization (NEDO) of Japan.

References

1. Del Campo C (2003) Pedicled or skeletonized? A review of the internal thoracic artery graft. Tex Heart Inst J 30:170–175
2. Castro GP, Dussin LH, Wender OB, Barbosa GV, Saadi EK (2005) Comparative analysis of the flows of left internal thoracic artery grafts dissected in the pedicled versus skeletonized manner for myocardial revascularization surgery. Arq Bras Cardiol 84:261–266
3. Deja MA, Woś S, Gołba KS, Zurek P, Domaradzki W, Bachowski R, Spyt TJ (1999) Intraoperative and laboratory evaluation of skeletonized versus pedicled internal thoracic artery. Ann Thorac Surg 68:2164–2168
4. Deja MA, Gołba KS, Malinowski M, Woś S, Kolowca M, Biernat J, Kajor M, Spyt TJ (2005) Skeletonization of internal thoracic artery affects its innervation and reactivity. Eur J Cardiothorac Surg 28:551–557
5. Wendler O, Tscholl D, Huang Q, Schäfers HJ (1999) Free flow capacity of skeletonized versus pedicled internal thoracic artery grafts in coronary artery bypass grafts. Eur J Cardiothorac Surg 15:247–250
6. Onorati F, Esposito A, Pezzo F, di Virgilio A, Mastroroberto P, Renzulli A (2007) Hospital outcome analysis after different techniques of left internal mammary grafts harvesting. Ann Thorac Surg 84:1912–1919
7. Takami Y, Ina H (2002) Effects of skeletonization on intraoperative flow and anastomosis diameter of internal thoracic arteries in coronary artery bypass grafting. Ann Thorac Surg 73:1441–1445
8. Austen WG, Edwards JE, Frye RL, Gensini GG, Gott VL, Griffith LS, McGoon DC, Murphy ML, Roe BB (1975) A reporting system on patients evaluated for coronary artery disease. Report of the Ad Hoc Committee for Grading of Coronary Artery Disease, Council on Cardiovascular Surgery, American Heart Association. Circulation 51:5–40
9. Kitamura K, Jorgensen CR, Gobel FL, Taylor HL, Wang Y (1972) Hemodynamic correlates of myocardial oxygen consumption during upright exercise. J Appl Physiol 32:516–522
10. Dönmez A, Tufan H, Tutar N, Araz C, Sezgin A, Karadeli E, Torgay A (2005) In vivo and in vitro effects of stellate ganglion blockade on radial and internal mammary arteries. J Cardiothorac Vasc Anesth 19:729–733
11. Baile EM, Paré PD, D'yachkova Y, Carere RG (1999) Effect of contrast media on coronary vascular resistance: contrast-induced coronary vasodilation. Chest 116:1039–1045
12. Evora PR, Pearson PJ, Discigil B, Oeltjen MR, Schaff HV (2002) Pharmacological studies on internal mammary artery bypass grafts. Action of endogenous and exogenous vasodilators and vasoconstrictors. J Cardiovasc Surg (Torino) 43:761–771
13. He GW, Yang CQ, Starr A (1995) Overview of the nature of vasoconstriction in arterial grafts for coronary operations. Ann Thorac Surg 59:676–683
14. Athanasiou T, Crossman MC, Asimakopoulos G, Cherian A, Weerasinghe A, Glenville B, Casula R (2004) Should the internal thoracic artery be skeletonized? Ann Thorac Surg 77:2238–2246
15. Higami T, Yamashita T, Nohara H, Iwahashi K, Shida T, Ogawa K (2001) Early results of coronary grafting using ultrasonically skeletonized internal thoracic arteries. Ann Thorac Surg 71:1224–1228
16. Cohen AJ, Lockman J, Lorberboym M, Bder O, Cohen N, Medalion B, Schachner A (1999) Assessment of sternal vascularity with single photon emission computed tomography after harvesting of the internal thoracic artery. J Thorac Cardiovasc Surg 118:496–502
17. Bonacchi M, Prifti E, Giunti G, Salica A, Frati G, Sani G (2001) Respiratory dysfunction after coronary artery bypass grafting employing bilateral internal mammary arteries: the influence of intact pleura. Eur J Cardiothorac Surg 19:827–833
18. Matsumoto M, Konishi Y, Miwa S, Minakata K (1997) Effect of different methods of internal thoracic artery harvest on pulmonary function. Ann Thorac Surg 63:653–655

19. Boodhwani M, Lam BK, Nathan HJ, Mesana TG, Ruel M, Zeng W, Sellke FW, Rubens FD (2006) Skeletonized internal thoracic artery harvest reduces pain and dysesthesia and improves sternal perfusion after coronary artery bypass surgery: a randomized, double-blind, within-patient comparison. Circulation 114:766–773

Journal of the American College of Cardiology
© 2010 by the American College of Cardiology Foundation
Published by Elsevier Inc.

Vol. 56, No. 19, 2010
ISSN 0735-1097/$36.00
doi:10.1016/j.jacc.2010.06.033

Augmented ST-Segment Elevation During Recovery From Exercise Predicts Cardiac Events in Patients With Brugada Syndrome

Hisaki Makimoto, MD,* Eiichiro Nakagawa, MD, PHD,† Hiroshi Takaki, MD, PHD,* Yuko Yamada MD,* Hideo Okamura, MD,* Takashi Noda, MD, PHD,* Kazuhiro Satomi, MD, PHD,* Kazuhiro Suyama, MD, PHD,* Naohiko Aihara, MD,* Takashi Kurita, MD, PHD,‡ Shiro Kamakura, MD, PHD,* Wataru Shimizu, MD, PHD*

Suita and Osaka, Japan

Objectives The goal of this study was to evaluate the prevalence and the clinical significance of ST-segment elevation during recovery from exercise testing.

Background During recovery from exercise testing, ST-segment elevation is reported in some patients with Brugada syndrome (BrS).

Methods Treadmill exercise testing was conducted for 93 patients (91 men), 46 ± 14 years of age, with BrS (22 documented ventricular fibrillation, 35 syncope alone, and 36 asymptomatic); and for 102 healthy control subjects (97 men), 46 ± 17 years of age. Patients were routinely followed up. The clinical end point was defined as the occurrence of sudden cardiac death, ventricular fibrillation, or sustained ventricular tachyarrhythmia.

Results Augmentation of ST-segment elevation ≥0.05 mV in V_1 to V_3 leads compared with baseline was observed at early recovery (1 to 4 min at recovery) in 34 BrS patients (37% [group 1]), but was not observed in the remaining 59 BrS patients (63% [group 2]) or in the 102 control subjects. During 76 ± 38 months of follow-up, ventricular fibrillation occurred more frequently in group 1 (15 of 34, 44%) than in group 2 (10 of 59, 17%; $p = 0.004$). Multivariate Cox regression analysis showed that in addition to previous episodes of ventricular fibrillation ($p = 0.005$), augmentation of ST-segment elevation at early recovery was a significant and independent predictor for cardiac events ($p = 0.007$), especially among patients with history of syncope alone (6 of 12 [50%] in group 1 vs. 3 of 23 [13%] in group 2) and among asymptomatic patients (3 of 15 [20%] in group 1 vs. 0 of 21 [0%] in group 2).

Conclusions Augmentation of ST-segment elevation during recovery from exercise testing was specific in patients with BrS, and can be a predictor of poor prognosis, especially for patients with syncope alone and for asymptomatic patients. (J Am Coll Cardiol 2010;56:1576–84) © 2010 by the American College of Cardiology Foundation

Brugada syndrome (BrS) is recognized as a clinical syndrome that leads to sudden cardiac death (SCD) in middle-aged persons due to ventricular fibrillation (VF) (1). Brugada syndrome is defined by a distinct 12-lead electrocardiogram (ECG) pattern in precordial leads (V_1 to V_3) presenting coved-type ST-segment elevation. Both depolarization and repolarization hypotheses have been reported for the pathogenesis of phenotype in BrS (2–5). Although several indexes have been reported as predictive factors of VF occurrence (6), the recent largest series of BrS patients suggested that there were no reliable predictors of cardiac events except for prior symptoms and spontaneous type 1 ECG (7). However, risk stratification remains disputable, especially for BrS patients without documented VF episodes.

See page 1585

Autonomic function has been suggested to relate to the occurrence of VF in BrS. It has also been shown that ST-segment elevation in patients with BrS was augmented

From the *Division of Arrhythmia and Electrophysiology, Department of Cardiovascular Medicine, National Cerebral and Cardiovascular Center, Suita, Japan; the †Department of Cardiology, Osaka City General Hospital, Osaka, Japan; and the ‡Division of Cardiology, Department of Internal Medicine, Kinki University School of Medicine, Osaka-Sayama, Osaka, Japan. Dr. Shimizu was supported in part by a research grant for the Cardiovascular Diseases (21C-8, 22-4-7) from the Ministry of Health, Labor and Welfare, Japan. All other authors have reported that they have no relationships to disclose.

Manuscript received April 21, 2010; revised manuscript received June 8, 2010, accepted June 15, 2010.

by selective stimulation of muscarinic receptors but mitigated by beta-adrenergic stimulation (8). Heart rate during exercise testing is considered as 1 parameter to evaluate cardiac autonomic function (9). Sympathetic withdrawal and parasympathetic activation occur at early recovery after exercise (10), which are expected to augment ST-segment elevation directly by inhibition of calcium-channel current or by decreasing heart rate (5,11). Two cases of BrS were reported in which ST-segment was augmented during and after exercise (12). Amin et al. (13) recently assessed the ECG responses to exercise in BrS patients with and without *SCN5A* mutations and control subjects. They reported that exercise resulted in an increase of peak J-point amplitude in all groups, including control subjects, and more QRS widening in BrS patients with *SCN5A* mutation. The peak J-point amplitude measured by Amin et al. (13) is thought to represent the depolarization parameter as QRS duration, or at least the combined parameter of both depolarization and repolarization. Therefore, in the present study, we measured several points of ST-segment as a repolarization parameter rather than a depolarization parameter, and tried to investigate the relationship between augmented ST-segment elevation during recovery from exercise testing and prognosis of BrS patients. We also evaluated parasympathetic reactivation by using heart rate recovery (HRR), which is defined as heart rate decay in the first minute after exercise cessation, and its relation with ST-segment change.

Methods

Study population. The study population consisted of 93 consecutive Japanese patients with BrS (91 males; mean age 46 ± 14 years) admitted to the National Cerebral and Cardiovascular Center in Suita, Japan, between 1994 and 2006. Ventricular fibrillation was documented in 22 BrS patients, syncope alone in 35 patients, and the remaining 36 patients were asymptomatic. As control subjects, 102 age-, sex-, and QRS duration-matched healthy subjects were randomly selected from persons who underwent treadmill exercise testing between 2002 and 2007 (97 males; mean age 46 ± 17 years). They included 55 normal subjects with normal QRS duration (<100 ms), 21 with incomplete right bundle branch block (RBBB) (100 ms ≤QRS duration <120 ms), and 26 with complete RBBB (120 ms ≤QRS duration) but without structural heart disease or any ventricular arrhythmias.

Brugada syndrome was diagnosed when a coved ST-segment elevation (≥0.2 mV at J-point) was observed in >1 of the right precordial leads (V_1 to V_3) in the presence or absence of a sodium-channel–blocking agent, and in conjugation with 1 of the following: documented VF, polymorphic ventricular tachycardia, family history of SCD <45 years of age, family history of BrS, inducibility of VF with programmed electrical stimulation, syncope, or an nocturnal agonal respiration (6). Structural heart diseases were carefully excluded by history taking, physical examinations, chest roentgenogram, ECG, and echocardiogram.

Abbreviations and Acronyms

AF = atrial fibrillation
BrS = Brugada syndrome
ECG = electrocardiogram
EPS = electrophysiologic study
HRR = heart rate recovery
ICD = implantable cardioverter-defibrillator
RBBB = right bundle branch block
RVOT = right ventricular outflow tract
SCD = sudden cardiac death
VF = ventricular fibrillation

Clinical, laboratory, electrocardiographic, and electrophysiologic study. The following clinical data were collected: family history of SCD (<45 years of age) or BrS, documented atrial fibrillation (AF), documented VF, syncope, age at the first cardiac event, and implantation of implantable cardioverter-defibrillator (ICD).

A 12-lead ECG was recorded in all 93 BrS patients, and RR interval, PR interval (lead II), QRS duration (lead V_5), corrected QT interval (lead V_2), QRS axis, J-point amplitude (leads V_2), and amplitude of several points of ST-segment (leads V_1, V_2, V_3) were measured.

Signal-averaged ECG was recorded and analyzed in 91 patients by using a signal-averaged ECG system (1200EPX, Arrhythmia Research Technology, Milwaukee, Wisconsin). Three parameters were assessed using a computer algorithm: 1) total filtered QRS duration; 2) root mean square voltage of the terminal 40 ms of the filtered QRS complexes (V_{40}); and 3) duration of low-amplitude signals <40 μV of the filtered QRS complexes (T_{40}). Late potential was considered present when the 2 criteria (V_{40} <18 μV and T_{40} >38 ms) were fulfilled.

Electrophysiologic study (EPS) was performed in 79 BrS patients (21 documented VF patients, 30 syncope alone patients, and 28 asymptomatic patients). A maximum of 3 programmed ventricular extrastimuli were delivered from the right ventricular apex and RVOT, unless VF was induced. No patients received antiarrhythmic drugs before EPS. The atrio-His and His-ventricular intervals were measured during sinus rhythm. The EPS was conducted after all subjects gave written informed consent.

Genetic testing for the presence of an *SCN5A* mutation was also conducted.

Exercise testing. Treadmill exercise testing was conducted in all 93 patients with BrS and 102 control subjects. Neither BrS patients nor control subjects used antiarrhythmic agents. A symptom-limited or submaximal (up to 90% of the age-predicted maximum heart rate) graded treadmill exercise testing similar to modified Bruce protocol was used. All 93 BrS patients and 102 control subjects were in normal sinus rhythm, and none had atrioventricular block at the exercise testing. The standard 12-lead ECGs were recorded at rest, at the end of each exercise stage, at peak exercise, and at every minute during recovery. The amplitude of ST-segment from the isoelectric line at the right precordial leads (V_1 to V_3 leads) and QRS width at V_5 lead were manually measured. The ST-segment point was defined as the point

JACC Vol. 56, No. 19, 2010
November 2, 2010:1576–84

where the vertical line from the end point of QRS at V_5 lead intersected the precordial leads. We also measured peak J-point amplitude in lead V_2 as a depolarization parameter, and amplitude of the point, which was 40 and 80 ms later than the peak J-points (ST40, ST80) in lead V_2 as a repolarization parameter. Measurements of ECG parameters were performed as the mean of 3 beats by single electrocardiologist who knew nothing about the patients. Significant augmentation of ST-segment elevation was defined as ST-segment amplitude increase ≥0.05 mV in at least 1 of V_1 to V_3 leads at early recovery (1 to 4 min at recovery) compared with the ST-segment amplitude at baseline (pre-exercise). We also recorded heart rate and blood pressure during exercise testing.

The HRR was defined as decay of heart rate from peak exercise to 1 min at recovery.

Follow-up. Follow-up was started after undergoing treadmill exercise testing. All patients with BrS were routinely followed up at the outpatient clinic of our hospital. The ICD implantation was performed in 63 BrS patients (20 documented VF patients, 25 syncope alone patients, and 18 asymptomatic patients). Antiarrhythmic drugs were prescribed for 7 patients; 2 patients who had episodes of VF but refused implantation of ICD (disopyramide 300 mg daily for 1 patient, and amiodarone 200 mg daily for another patient), 2 patients who had AF (quinidine 300 mg daily), and 3 patients who had previous history of both VF and AF and implanted ICD (quinidine 300 mg daily for 1 patient, amiodarone 200 mg daily for 2 patients).

Cardiac events were defined as SCD or aborted cardiac arrest, and VF or sustained ventricular tachyarrhythmia documented by ICD or ECG recordings.

Statistical analysis. Data were analyzed with Dr. SPSS II for Windows software package (SPSS Inc., Chicago, Illinois). Numeric values are expressed as mean ± SD. The chi-square test, Student *t* test, or 1-way analysis of variance was performed when appropriate to test for statistical differences. All p values <0.05 were considered statistically significant. Event rate curves were plotted according to the Kaplan-Meier method, and were analyzed with the log-rank test. Univariate and multivariate Cox regression were performed to assess whether 7 indexes can be significant and independent predictors of subsequent cardiac events. We used the forward step-wise approach with p to enter a value of 0.05 for multivariate analysis. Augmentation of ST-segment elevation at early recovery, family history of SCD or BrS, spontaneous coved-type ST-segment elevation, presence of *SCN5A* mutation, late potential, VF inducibility during EPS, and previous episodes of VF were included as indexes.

Results

There were no significant differences between 93 BrS patients and 102 control subjects with respect to age at exercise testing, sex, QRS duration (lead V_5), and QTc interval (lead V_2), as summarized in Table 1. The RR interval and PR interval (lead II) were significantly longer in BrS patients than in control subjects.

Table 1 Initial Characteristics of Patients and Control Subjects

	Brugada Patients (n = 93)	Control Subjects (n = 102)	p Value
Age at exercise testing, yrs	46 ± 14	46 ± 17	NS
Sex, male	91 (98%)	97 (95%)	NS
Electrocardiographic characteristics, ms			
RR	952 ± 151	903 ± 140	0.020
PR	178 ± 30	165 ± 24	0.001
QRS duration	98 ± 16	98 ± 20	NS
QTc	416 ± 44	406 ± 30	NS

Values are mean ± SD or n (%).
QTc = corrected QT interval.

Response of ST-segment elevation during treadmill exercise testing. Among 93 BrS patients, significant augmentation of ST-segment elevation mostly associated with coved pattern at early recovery phase was observed in 34 BrS patients (37% [group 1]), but not in the remaining 59 BrS patients (63% [group 2]). Conversely, ST-segment augmentation was never observed in any of the 102 control subjects (34 of 93 [37%] vs. 0 of 102 [0%], $p < 0.0001$). Typical responses of ST-segment amplitudes of 3 groups are shown in Figure 1. Composite data of serial changes of ST-segment amplitude in V_1 and V_2 leads during exercise testing are illustrated in Figure 2A. The serial changes of ST-segment amplitude in V_3 lead showed the same trend (not shown). In group 1, ST-segment amplitude decreased at peak exercise and started to reascend at early recovery, and culminated at 3 min of recovery (Figs. 1A and 2A). In contrast, ST-segment amplitude of group 2 patients and control subjects decreased at peak exercise, and gradually returned to the baseline amplitude rather than showing augmentation (Figs. 1B to 1D and 2A). Significant differences were identified between group 1 and group 2 patients in the ST-segment amplitude in leads V_1 and V_2 from peak exercise to 6 min of recovery, whereas no major differences were observed between group 2 patients and control subjects (Fig. 2A). Composite data of serial changes of peak J-point amplitude, ST40, and ST80 amplitudes are presented in Figure 2B. The peak J-point amplitude and ST40 amplitude during recovery showed the same trend as the ST-segment amplitude in Figure 2A. Significant differences were identified between group 1 and group 2 patients in the peak J-point and ST40 amplitudes from peak exercise to 6 min of recovery. The ST80 amplitude showed significant differences between group 1 and group 2 patients at 2, 3, and 4 min of recovery. At peak exercise, the peak J-point amplitude increased in 34 (37%) of 93 Brugada patients and in 26 (26%) of 102 control subjects, although the ST-segment

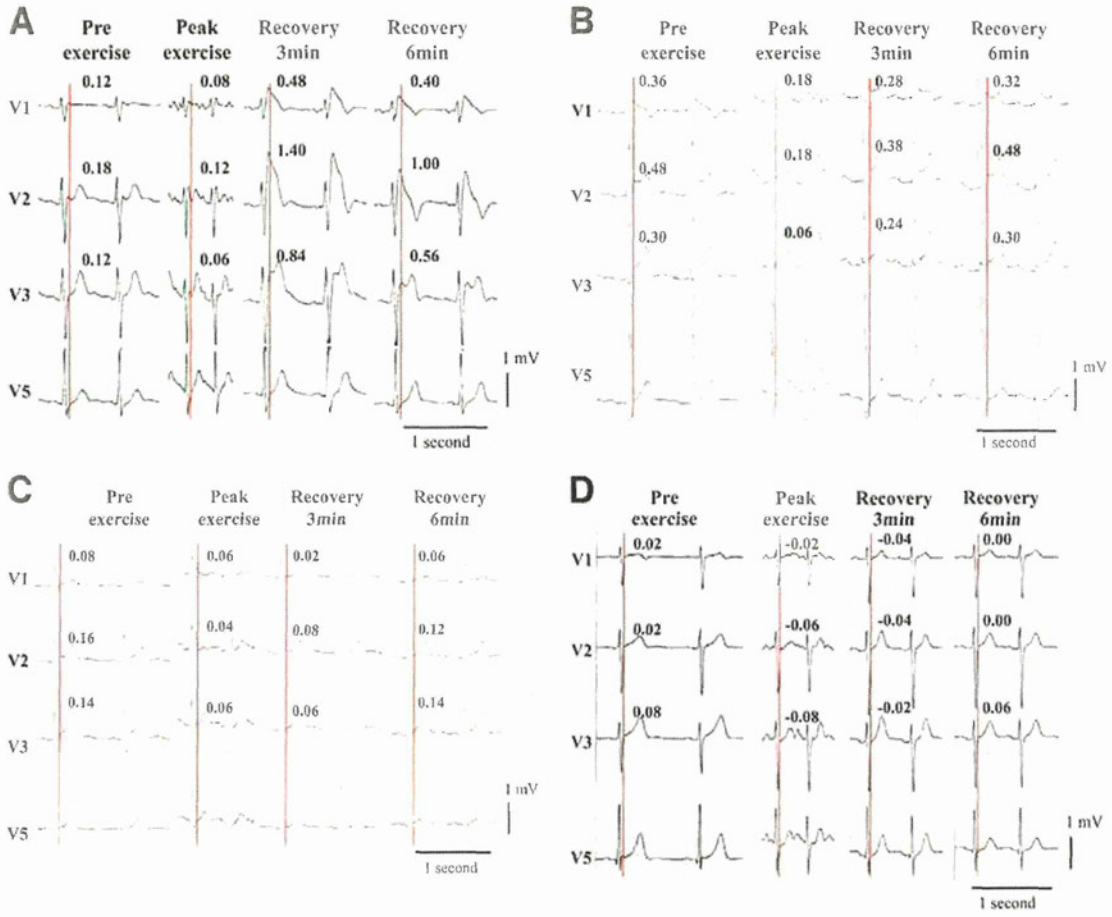

Figure 1 **Typical Responses of ST-Segment Amplitude in Leads V_1, V_2, V_3, and V_5 During Exercise Testing in Brugada Syndrome Patients**

(A) In the group 1 Brugada patient showing saddle-back type ST-segment (lead V_2) at baseline, ST-segment amplitude slightly decreased at peak exercise, but rea-scended at early recovery (3 min), resulting in typical coved-type ST-segment elevation. **(B, C)** In the group 2 Brugada patient and **(D)** in the control subject, ST-segment amplitude decreased at peak exercise and gradually recovered to the baseline at recovery. It is noteworthy that the peak J-point amplitude in lead V_2 was augmented despite not showing ST-segment augmentation in **A** and **C**. The ST-segment amplitudes are shown as numeric values expressed in millivolts (mV). The **red vertical line** indicates the line from the end point of the QRS interval at electrocardiography lead V_5.

amplitude and ST40 amplitude decreased in most patients of both groups.

Comparison of HRR is shown in Figure 3. The HRR of group 1 patients was significantly larger than that of group 2 patients (32 ± 15 vs. 23 ± 10, p = 0.0007) and control subjects (32 ± 15 vs. 26 ± 10, p = 0.021). The differences of HRR between group 2 patients and control subjects were also statistically significant (23 ± 10 vs. 26 ± 10, p = 0.026).

Although there were no sustained or nonsustained ventricular arrhythmias throughout exercise testing, single premature ventricular complexes were observed during exercise in 8 of the group 1 patients and in 11 of the group 2 patients, and at recovery in 10 of the group 1 patients and in 9 of the group 2 patients. There were no significant differences between groups 1 and 2 in incidences of premature ventricular complexes.

Clinical, laboratory, electrocardiographic, and electrophysiologic characteristics. Comparison of the clinical, laboratory, electrocardiographic, and electrophysiologic characteristics between groups 1 and 2 patients are shown in Table 2. There were no significant differences in these characteristics between groups 1 and 2 except for the presence of *SCN5A* mutation and late potential (*SCN5A* mutation, 17% vs. 5%, p = 0.048; late potential, 82% vs. 53%, p = 0.004).

Follow-up. The mean follow-up period for the 93 BrS patients was 75.7 ± 38.4 months. During follow-up, 25 of all 93 BrS patients (27%) had cardiac events, and the incidence of cardiac events was significantly higher in group 1 than in group 2 patients (44% vs. 17%, p = 0.004). The period from exercise testing to cardiac events ranged from 1 to 78 months (median 12 months). One patient in group 2, who refused implantation of ICD and was taking disopyr-

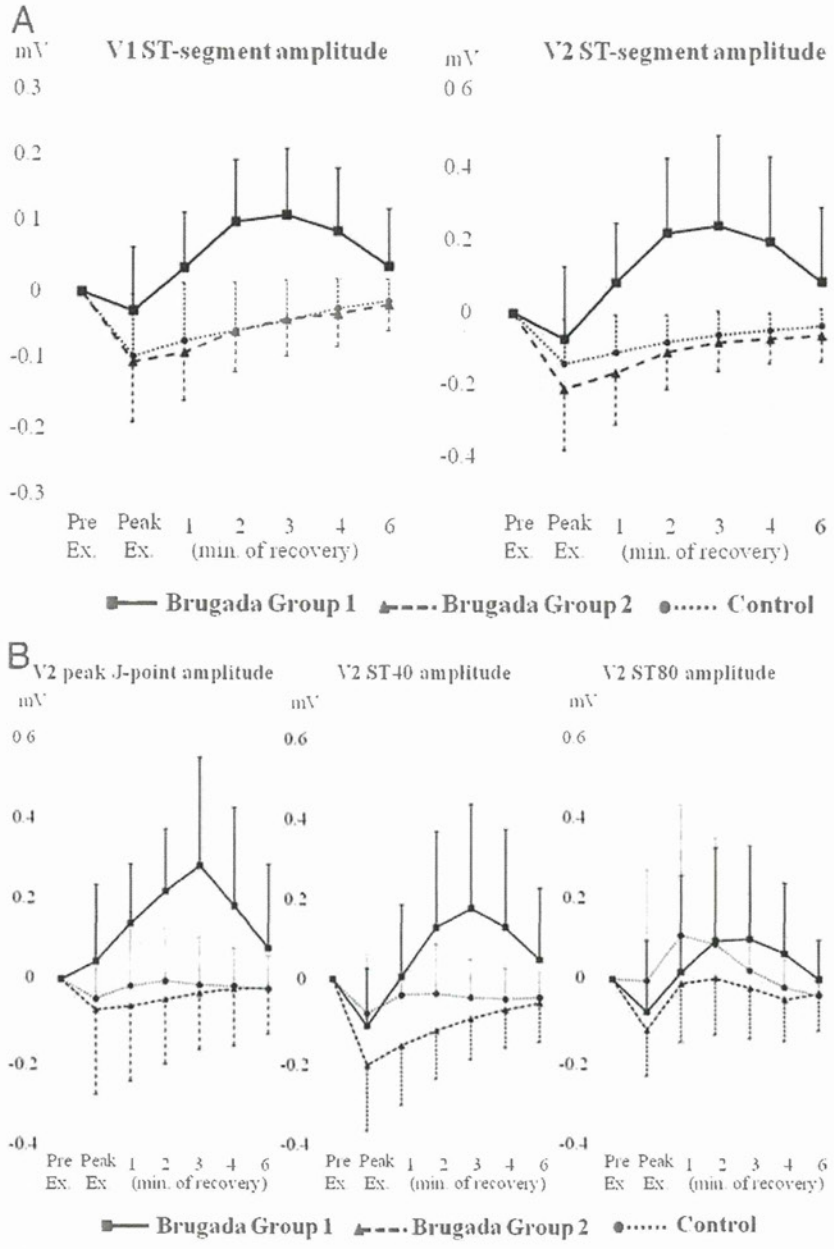

Figure 2 **Composite Data of Serial Changes of ST-Segment Amplitude**

(A) Composite data of serial changes of ST-segment amplitude in lead V_1 **(left)** and lead V_2 **(right)** during exercise (Ex.) testing in group 1 Brugada syndrome patients **(squares)** and group 2 Brugada syndrome patients **(triangles)**, and in control subjects **(circles)**. **(B)** Peak J-point amplitude **(left)**, ST40 amplitude **(middle)**, and ST80 amplitude **(right)** in lead V_2. The ST-segment amplitude decreased at peak exercise and started to reascend at early recovery, and culminated at 3 min of recovery in group 1 Brugada patients. In the group 2 Brugada patients and control subjects, the ST-segment amplitude decreased at peak exercise and gradually recovered to the baseline level during recovery. The peak J-point amplitude and ST40 amplitude during recovery showed the same trend as the ST-segment amplitude. Since ST80 amplitude was influenced by T wave, especially at rapid heart rate, the trends of the 3 groups were somewhat different from ST-segment amplitude or ST40 amplitude. The ST-segment amplitudes are shown as values compared to pre-exercise ST-segment amplitudes. $p < 0.05$.

amide 300 mg daily, died of VF. Three of 7 patients with medication had cardiac events, including 1 death.

Predictors of outcome. Kaplan-Meier analysis demonstrated significant differences in the time to the first cardiac event depending on the presence of ST-segment augmentation during recovery from exercise (Fig. 4A). Group 1 patients had a significantly higher cardiac event rate than group 2 patients (log-rank, $p = 0.0029$). Previous history of VF (Fig. 4B) and positive *SCN5A* mutation (Fig. 4C) also had significant values for occurrence of subsequent cardiac events ($p = 0.0013$ and $p = 0.028$, respectively); however, spontaneous coved-type ST-segment elevation did not predict cardiac events ($p =$

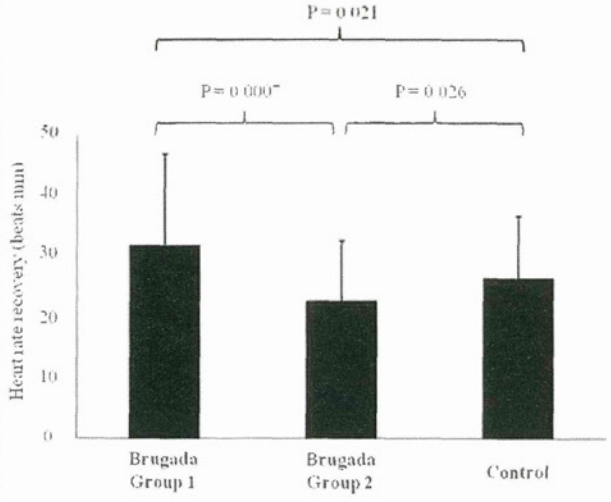

Figure 3 **Comparison of HRR After Exercise Cessation**

Comparison of heart rate recovery (HRR) 1 min after exercise cessation among Brugada syndrome patients of groups 1 and 2 and control subjects. The HRR in group 1 patients was significantly larger than that in group 2 (32 ± 15 beats/min vs. 23 ± 10 beats/min, p = 0.0007) and in control subjects (32 ± 15 beats/min vs. 26 ± 10 beats/min, p = 0.021). The differences of HRR between group 2 patients and control subjects were also significant (23 ± 10 beats/min vs. 26 ± 10 beats/min, p = 0.026).

0.068) (Fig. 4D). The results of Cox regression analysis are shown in Table 3. In univariate analysis, indexes predictive of cardiac events were previous episodes of VF (p = 0.003), ST-segment augmentation at early recovery (group 1; p = 0.005), and presence of *SCN5A* mutation (p = 0.037). In multivariate Cox regression analysis, previous episodes of VF and ST-segment augmentation at early recovery were significant and independent predictors of subsequent cardiac events (p = 0.005 and p = 0.007, respectively).

The incidence of cardiac events during follow-up in the subgroups according to symptoms before exercise testing is shown in Table 4. In the subgroup of 35 BrS patients with syncope alone, group 1 had a significantly higher cardiac event rate than group 2 (log-rank, 6 of 12 [50%] vs. 3 of 23 [13%], p = 0.016). Of note, among 36 asymptomatic patients, only 3 patients (9%) in group 1 experienced cardiac events. The log-rank test also demonstrated higher cardiac event risk in group 1 compared with group 2 (3 of 15 [20%] vs. 0 of 21 [0%], p = 0.039).

Discussion

The major findings of the present study were the following: 1) 37% of BrS patients showed ST-segment augmentation at early recovery during exercise testing; 2) ST-segment augmentation at early recovery was specific in BrS patients, and was significantly associated with a higher cardiac event rate, notably for patients with previous episode of syncope or for asymptomatic patients; and 3) BrS patients with ST-segment augmentation at early recovery showed significantly larger HRR. This is the first systematic report on the relationship between ST-segment augmentation during recovery from exercise and prognosis for BrS patients.

Augmentation of ST-segment elevation and possible mechanism. It is well known that autonomic function influences an extent of ST-segment elevation in BrS (8). The ST-segment elevation is mitigated by administration of β-adrenergic agonists and is enhanced by parasympathetic agonists such as acetylcholine in experimental and clinical investigations (5,14–16). Parasympathetic reactivation is thought to occur at early recovery after treadmill exercise testing, especially in the first minute after cessation of exercise (10,17). In the present study, we measured the ST-segment amplitude as a repolarization parameter rather than a depolarization parameter, and evaluated HRR to investigate the correlation between ST-segment augmentation and parasympathetic activity (9,18). The BrS patients who had ST-segment augmentation had significantly larger HRR compared with patients who did not, suggesting that the ST-segment augmentation was closely related to higher parasympathetic activity. However, it is still unclear whether ST-segment augmentation observed in the 34 BrS patients was simply due to more increased parasympathetic activity or to more increased susceptibility (hypersensitivity) to the parasympathetic reactivation.

Conversely, the *SCN5A* mutation was more frequently identified in group 1. Scornik et al. (19) reported that *SCN5A* mutation can accentuate parasympathetic activity toward the heart directly. It was also reported that specific mutations in the *SCN5A* gene may lead to augmentation of J-point amplitude or ST-segment amplitude during beta-adrenergic stimulation (20,21). Veldkamp et al. (20) demonstrated that a specific *SCN5A* mutation, 1795insD, augments slow inactivation, and delays recovery of sodium channel availability, thus reducing the sodium current and resulting in augmented peak J-point amplitude at rapid heart rate. Increased body temperature induced by exercise can be a risk of life-threatening arrhythmias in patients with BrS (22). A specific *SCN5A* missense mutation, T1620M, was reported to cause a faster decay of the sodium channel but slower recovery from inactivation, resulting in increased ST-segment elevation in precordial leads at higher temperatures during exercise. Although Amin et al. (13) reported that exercise induced augmentation of peak J-point amplitude, a depolarization parameter or at least combined parameter of both depolarization and repolarization, in all subjects tested, the incidence of increase in the peak J-point amplitude at peak exercise was lower (37%) in our Brugada patients. This is probably in part because only 9 (10%) of our 93 BrS patients had the *SCN5A* mutation. We could not identify significant differences in HRR, QRS duration, peak J-point amplitude (lead V_2), and ST-segment amplitude (leads V_1, V_2, V_3) at peak exercise between patients with and without *SCN5A* mutation (not shown), and that may be also due to the small number of BrS patients with *SCN5A* mutation.

Risk stratification in BrS. Implantation of an ICD is a first line of therapy for secondary prevention in patients with BrS who exhibited previous history of VF. The American College

JACC Vol. 56, No. 19, 2010
November 2, 2010:1576–84

Table 2 Clinical, Laboratory, Electrocardiographic, and Electrophysiologic Characteristics and Long-Term Follow-Up of Groups 1 and 2 Brugada Syndrome Patients

Characteristic	Group 1 (n = 34)	Group 2 (n = 59)	p Value
Clinical characteristics			
Age at exercise testing, yrs	42 ± 11	48 ± 15	NS
Men	34 (100%)	57 (97%)	NS
Family history of SCD at age <45 yrs or Brugada syndrome	7 (21%)	16 (27%)	NS
Documented AF	7 (21%)	12 (20%)	NS
Documented VF before exercise testing	7 (21%)	15 (25%)	NS
Syncope alone before exercise testing	12 (35%)	23 (39%)	NS
Asymptomatic before exercise testing	15 (44%)	21 (36%)	NS
Age at first cardiac event, yrs	42 ± 13	45 ± 15	NS
ICD implantation	25 (74%)	38 (64%)	NS
Laboratory characteristics			
SCN5A mutation	6 (17%)	3 (5%)	0.048
Electrocardiographic characteristics			
RR, ms	951 ± 170	953 ± 140	NS
PR, ms	184 ± 28	175 ± 31	NS
QRS, ms	98 ± 14	98 ± 17	NS
QTc, ms	418 ± 46	415 ± 43	NS
ST-segment amplitude (mV) at baseline			
V_1	0.14 ± 0.09	0.16 ± 0.12	NS
V_2	0.41 ± 0.22	0.38 ± 0.26	NS
V_3	0.22 ± 0.13	0.19 ± 0.14	NS
Spontaneous coved-type ST-segment elevation in right precordial leads	30 (88%)	43 (73%)	NS
Signal-averaged electrocardiogram			
TfQRS, ms	122 ± 15	118 ± 17	NS
Late potential	28/34 (82%)	30/57 (53%)	0.004
Premature ventricular complexes during exercise	8 (24%)	11 (19%)	NS
Premature ventricular complexes at recovery	10 (29%)	9 (15%)	NS
Electrophysiologic characteristics			
AH interval, ms	107 ± 24	98 ± 27	NS
HV interval, ms	45 ± 8	44 ± 11	NS
Induction of VF	26/31 (84%)	33/47 (70%)	NS
Follow-up			
Cardiac events	15 (44%)	10 (17%)	0.004
Follow-up period, months	74.1 ± 42.2	76.5 ± 36.4	NS

AF = atrial fibrillation; ICD = implantable cardioverter-defibrillator; SCD = sudden cardiac death; TfQRS = total filtered QRS duration; VF = ventricular fibrillation; other abbreviations as in Table 1.

of Cardiology/American Heart Association/Heart Rhythm Society guidelines refer to BrS patients who have had syncope as having Class IIa indication for ICD therapy (23). However, there is still much room for argument with respect to treatments for patients who have had only syncope, and for asymptomatic patients (24–28). Although inducibility of VF during EPS (25,26), family history of SCD (24), spontaneous type 1 ECG (25,27), and late potential (28) have been proposed as predictors of cardiac events, the availability of these indexes remains controversial (7,29).

In the present study, a previous episode of VF (or aborted cardiac arrest) was the strongest predictor of subsequent cardiac events, as in previous studies (7,30,31). Moreover, ST-segment augmentation at early recovery during exercise testing was a significant and independent predictor of subsequent cardiac events in the present study. The results suggested that parasympathetic activity plays an important role in both ST-segment augmentation and subsequent cardiac events. As previously noted, it remains unclear that the cause of ST-segment augmentation in our 34 patients was a result of more increased parasympathetic activity or of more increased susceptibility of the patients to the increased parasympathetic reactivation.

Study limitations. First, BrS patients were confined to those who were hospitalized in our hospital for close investigation. That indicates these patients can be biased toward relatively high risk. Second, the present study is based on data from a small population of 93 patients; hence, it was not sufficient to evaluate the prognosis, and there also was a small number of events. Although we adopted a step-wise approach, the limited number of events can lessen the precision of the consequences for multivariate Cox regression analysis.

Conclusions

The presence of *SCN5A* mutation was a significant predictor of subsequent cardiac events by univariate Cox regression analysis. However, multivariate Cox regression analysis showed it was not a significant predictor of prognosis.

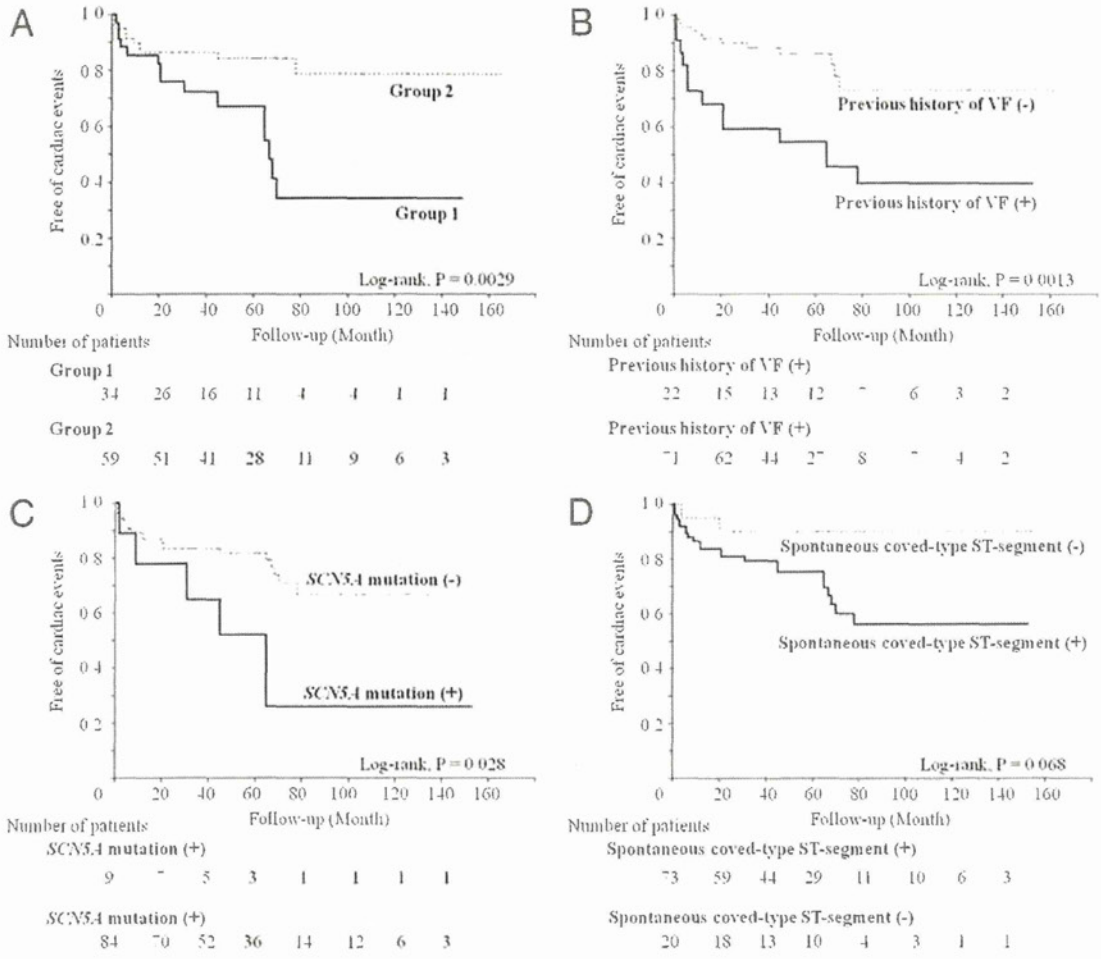

Figure 4 **Kaplan-Meier Analysis of Cardiac Events During Follow-Up**

Kaplan-Meier analysis of **(A)** cardiac events during follow-up, depending on patterns in response to ST-segment elevation during exercise test (groups 1 and 2), **(B)** incidence of previous episode of ventricular fibrillation (VF), **(C)** *SCN5A* mutation, and **(D)** spontaneous coved-type ST-segment elevation. Group 1 Brugada patients had a significantly higher cardiac event rate than did group 2 Brugada patients (log-rank, p = 0.0029). Brugada patients with previous episodes of VF or with *SCN5A* mutation had significantly greater values for occurrence of subsequent cardiac events than did patients without VF episodes or *SCN5A* mutation (p = 0.0013, p = 0.028, respectively), whereas spontaneous coved-type ST-segment elevation in Brugada patients did not predict cardiac events compared with patients not having such ST-segment elevation (p = 0.068).

Further study with a larger number of BrS patients will be required to evaluate the significance of the index as a predictor of subsequent cardiac events.

As for BrS patients with only syncope, subsequent cardiac events occurred in 50% (6 of 12) patients who exhibited ST-segment augmentation at early recovery. Asymptomatic

Table 3 **Predictive Capabilities of Cardiac Events**

		Univariate Analysis		Multivariate Analysis	
	Positive, n (%)	HR (95% CI)	p Value	HR (95% CI)	p Value
Previous episodes of VF	22 (24%)	3.40 (1.54–7.53)	0.003	3.25 (1.43–7.37)	0.005
Augmentation of ST-segment elevation at early recovery phase	34 (37%)	3.17 (1.42–7.09)	0.005	3.17 (1.37–7.33)	0.007
SCN5A mutation	9 (10%)	2.86 (1.07–7.66)	0.037		
Spontaneous coved-type ST-segment	72 (77%)	3.51 (0.83–14.9)	0.089		
Late potential	58/91 (64%)	2.25 (0.84–5.99)	0.11		
VF inducible in EPS	59/78 (76%)	0.73 (0.30–1.75)	0.48		
Family history of SCD or BrS	23 (25%)	1.19 (0.47–3.02)	0.72		

BrS = Brugada syndrome; CI = confidence interval; EPS = electrophysiologic study; HR = hazard ratio; other abbreviations as in Table 2.

Table 4 Incidence of Cardiac Events According to Symptoms Before Exercise Testing

Type	n	Treadmill Exercise Test	n	VF Occurrence	p Value (vs. Group 1)
Documented VF	**22**	Group 1	7	6 (86%)	
		Group 2	15	7 (47%)	0.14
Syncope alone	35	Group 1	12	6 (50%)	
		Group 2	23	3 (13%)	0.016
Asymptomatic	**36**	Group 1	15	3 (20%)	
		Group 2	21	0 (0%)	0.039

The p value was calculated according to the log-rank test.
VF = ventricular fibrillation.

patients who had ST-segment augmentation at early recovery had a higher incidence of cardiac events than patients who did not. These data suggested the potential utility of exercise testing to predict cardiac events for patients with BrS who have had previous episodes of only syncope but not VF or who have had no symptoms.

Reprint requests and correspondence: Dr. Wataru Shimizu, Division of Arrhythmia and Electrophysiology, Department of Cardiovascular Medicine, National Cerebral and Cardiovascular Center, 5-7-1 Fujishiro-dai, Suita, Osaka 565-8565, Japan. E-mail: wshimizu@hsp.ncvc.go.jp.

REFERENCES

1. Brugada P, Brugada J. Right bundle branch block, persistent ST segment elevation and sudden cardiac death: a distinct clinical and electrocardiographic syndrome: a multicenter report. J Am Coll Cardiol 1992;20:1391–6.
2. Smits JP, Eckardt L, Probst V, et al. Genotype-phenotype relationship in Brugada syndrome: electrocardiographic features differentiate *SCN5A*-related patients from non-*SCN5A*-related patients. J Am Coll Cardiol 2002;40:350–6.
3. Tukkie R, Sogaard P, Vleugels J, de Groot IK, Wilde AA, Tan HL. Delay in right ventricular activation contributes to Brugada syndrome. Circulation 2004;109:1272–7.
4. Shimizu W, Aiba T, Kamakura S. Mechanisms of disease: current understanding and future challenges in Brugada syndrome. Nat Clin Pract Cardiovasc Med 2005;2:408–14.
5. Yan GX, Antzelevitch C. Cellular basis for the Brugada syndrome and other mechanisms of arrhythmogenesis associated with ST-segment elevation. Circulation 1999;100:1660–6.
6. Antzelevitch C, Brugada P, Borggrefe M, et al. Brugada syndrome. Report of the second consensus conference: endorsed by the Heart Rhythm Society and the European Heart Rhythm Association. Circulation 2005;111:659–70.
7. Probst V, Veltmann C, Eckardt L, et al. Long-term prognosis of patients diagnosed with Brugada syndrome: results from the FINGER Brugada syndrome registry. Circulation 2010;121:635–43.
8. Miyazaki T, Mitamura H, Miyoshi S, Soejima K, Aizawa Y, Ogawa S. Autonomic and antiarrhythmic drug modulation of ST segment elevation in patients with Brugada syndrome. J Am Coll Cardiol 1996;27:1061–70.
9. Lahiri MK, Kannankeril PJ, Goldberger JJ. Assessment of autonomic function in cardiovascular disease. J Am Coll Cardiol 2008;51:1725–33.
10. Arai Y, Saul JP, Albrecht P, et al. Modulation of cardiac autonomic activity during and immediately after exercise. Am J Physiol 1989;256: H132–41.
11. Litovsky SH, Antzelevitch C. Differences in the electrophysiological response of canine ventricular subendocardium and subepicardium to acetylcholine and isoproterenol. A direct effect of acetylcholine in ventricular myocardium. Circ Res 1990;67:615–27.
12. Papadakis M, Petzer E, Sharma S. Unmasking of the Brugada phenotype during exercise testing and its association with ventricular arrhythmia on the recovery phase. Heart 2009;95:2022.
13. Amin AS, de Groot EA, Ruijter JM, Wilde AA, Tan HL. Exercise-induced ECG changes in Brugada syndrome. Circ Arrhythm Electrophysiol 2009;2:531–9.
14. Noda T, Shimizu W, Taguchi A, et al. ST-segment elevation and ventricular fibrillation without coronary spasm by intracoronary injection of acetylcholine and/or ergonovine maleate in patients with Brugada syndrome. J Am Coll Cardiol 2002;40:1841–7.
15. Ikeda T, Abe A, Yusu S, et al. The full stomach test as a novel diagnostic technique for identifying patients at risk of Brugada syndrome. J Cardiovasc Electrophysiol 2006;17:602–7.
16. Yokokawa M, Okamura H, Noda T, et al. Neurally-mediated syncope as a cause of syncope in patients with Brugada electrocardiogram. J Cardiovasc Electrophysiol 2010;21:186–92.
17. Savin WM, Davidson DM, Haskell WL. Autonomic contribution to heart rate recovery from exercise in humans. J Appl Physiol 1982;53: 1572–5.
18. Imai K, Sato H, Hori M, et al. Vagally mediated heart rate recovery after exercise is accelerated in athletes but blunted in patients with chronic heart failure. J Am Coll Cardiol 1994;24:1529–35.
19. Scornik FS, Desai M, Brugada R, et al. Functional expression of "cardiac-type" Nav1.5 sodium channel in canine intracardiac ganglia. Heart Rhythm 2006;3:842–50.
20. Veldkamp MW, Viswanathan PC, Bezzina C, Baartscheer A, Wilde AA, Balser JR. Two distinct congenital arrhythmias evoked by a multidysfunctional Na+ channel. Circ Res 2000;86:e91–7.
21. Clancy CE, Rudy Y. Na^+ channel mutation that causes both Brugada and long-QT syndrome phenotypes. A stimulation study of mechanism. Circulation 2002;105:1208–13.
22. Dumaine R, Towbin JA, Brugada P, et al. Ionic mechanisms responsible for the electrocardiographic phenotype of the Brugada syndrome are temperature dependent. Circ Res 1999;85:803–9.
23. Epstein AE, Dimarco JP, Ellenbogen KA, et al. ACC/AHA/HRS 2008 guidelines for device-based therapy of cardiac rhythm abnormalities: a report of the American College of Cardiology/American Heart Association Task Force on Practice Guidelines (Writing Committee to Revise the ACC/AHA/NASPE 2002 Guideline Update for Implantation of Cardiac Pacemakers and Antiarrhythmia Devices). J Am Coll Cardiol 2008;51:e1–62.
24. Kamakura S, Ohe T, Nakazawa K, et al., for the Brugada Syndrome Investigators in Japan. Long-term prognosis of probands with Brugada-pattern ST-elevation in leads V1-V3. Circ Arrhythm Electrophysiol 2009;2:495–503.
25. Brugada J, Brugada R, Antzelevitch C, Towbin J, Nademanee K, Brugada P. Long term follow-up of individuals with the electrocardiographic pattern of right bundle-branch block and ST-segment elevation in precordial leads V1 to V3. Circulation 2002;105:73–8.
26. Brugada P, Brugada R, Mont L, Rivero M, Geelen P, Brugada J. Natural history of Brugada syndrome: the prognostic value of programmed electrical stimulation of the heart. J Cardiovasc Electrophysiol 2003;14:455–7.
27. Priori SG, Napolitano C, Gasparini M, et al. Natural history of Brugada syndrome: insights for risk stratification and management. Circulation 2002;105:1342–7.
28. Ikeda T, Takami M, Sugi K, Mizusawa Y, Sakurada H, Yoshino H. Noninvasive risk stratification of subjects with a Brugada-type electrocardiogram and no history of cardiac arrest. Ann Noninvasive Electrocardiol 2005;10:396–403.
29. Paul M, Gerss J, Schulze-Bahr E, et al. Role of programmed ventricular stimulation in patients with Brugada syndrome: a meta-analysis of worldwide published data. Eur Heart J 2007;17:2126–33.
30. Eckardt L, Probst V, Smits JP, et al. Long-term prognosis of individuals with right precordial ST-segment-elevation Brugada syndrome. Circulation 2005;111:257–63.
31. Sacher F, Probst V, Iesaka Y, et al. Outcome after implantation of a cardioverter-defibrillator in patients with Brugada syndrome: a multicenter study. Circulation 2006;114:2317–24.

Key Words: Brugada syndrome ■ exercise testing ■ ST-segment elevation.

Subtraction Magnetocardiogram for Detecting Coronary Heart Disease

Akihiko Kandori, Ph.D.,* Kuniomi Ogata,* Tsuyoshi Miyashita, M.S.,* Hiroshi Takaki, Ph.D., M.D.,† Hideyuki Kanzaki, Ph.D., M.D.,† Syuji Hashimoto,† Wataru Shimizu, Ph.D., M.D.,† Shiro Kamakura, Ph.D., M.D.,† Shigeyuki Watanabe, Ph.D., M.D.,‡ and Kazutaka Aonuma, Ph.D.‡

*From the *Advanced Research Laboratory, Kokubunji, Tokyo, Japan; †National Cardiovascular Center, Osaka, Japan; and ‡University of Tsukuba, Ibaraki, Japan*

Background: A large-scale magnetocardiogram (MCG) database was produced, and standard MCG waveforms of healthy patients were calculated by using this database. It was clarified that the standard MCG waveforms are formed with the same shape and current distribution in healthy patients. A new subtraction method for detecting abnormal ST-T waveforms in coronary heart disease (CHD) patients by using the standard MCG waveform was developed.

Methods: We used MCGs of 56 CHD patients (63 ± 3 years old) and 101 age-matched normal control patients (65 ± 5 years old). To construct a subtracted ST-T waveform, we used standard MCG waveforms produced from 464 normal MCGs (male: 268, female: 196). The standard MCG waveforms were subtracted from each subject's measured MCGs, which were shortened or lengthened and normalized to adjust to the data length and magnitude of the standard waveform. We evaluated the maximum amplitude and maximum current-arrow magnitude of the subtracted ST-T waveform.

Results: The maximum magnetic field, maximum magnitude of current arrows, and maximum magnitude of total current vector increased according to the number of coronary artery lesions. The sensitivity and specificity of detecting CHD and normal control patients were 74.6% and 84.1%, respectively.

Conclusions: The subtraction MCG method can be used to detect CHD with high accuracy, namely, sensitivity of 74.6% and specificity of 84.1% (in the case of maximum amplitude of total current vector). Furthermore, the subtraction MCG magnitude and its current distribution can reflect the expanse of the ischemic lesion area and the progress from ischemia to myocardial infarction.

Ann Noninvasive Electrocardiol 2010;15(4):360–368

magnetocardiogram; subtraction; current-arrow map; Coronary Heart Disease

INTRODUCTION

Coronary heart disease (CHD) is the most common cause of death in the world. Advances in noninvasive coronary-artery imaging, such as x-ray coronary angiography[1] and multidetector computed tomography (CT),[1,2] has enabled early and precise detection of CHD. These tools are needed to treat artery constriction and improve the symptoms of angina. On the other hand, as functional tests of myocardial activity, exercise electrocardiogram (ECG) and single-photon-emission computed tomography (SPECT) are widely used for detecting signs of cardiac sudden death in CHD patients.[3,4] However, the distribution of myocardial electrical currents, which include information on damaged tissues, cannot be detected with these cardiac tests.

Noncontact magnetocardiograms (MCGs) can produce a myocardial-current-distribution map by detecting weak magnetic fields generated by myocardial electrical currents. The morphology of MCG waveforms produced from electrical currents is similar for each person because the MCG signals are less affected by organ conductivity, and the

Address for correspondence: Akihiko Kandori, Advanced Research Laboratory, Hitachi Ltd., 1-280 Higashi-Koigakubo, Kokubunji, Tokyo 185-8601, Japan. Fax: +81-42-327-7783; E-mail: akihiko.kandori.vc@hitachi.com

Sources of financial support: None.

two-dimensional currents in the heart only produce a magnetic field. Given those facts, we constructed a database of 464 adult healthy patients[5] and a template MCG waveform.[6] In particular, the database and template enable the normal activity in the ST-T wave to be subtracted because of calm repolarization. Furthermore, some researchers have reported high CHD detection sensitivity[7–15] when MCGs are used because the ST-T MCG waves of CHD patients have an abnormal pattern. And MCGs are useful in detecting myocardial infarction (MI) in non-ST-segment elevation.[14,15]

To detect ST-T abnormality in CHD patients, we used our MCG-waveform template to construct a subtraction ST-T waveform. Subtraction of ST-T waveforms of CHD patients and control patients is used to evaluate the efficacy of detecting CHD, the difference between electrical current abnormalities in lesion areas, and the difference between ischemia and MI.

METHODS

Participants

Fifty-six Japanese CHD patients (10 females and 46 males) and 101 Japanese normal control patients (31 females and 70 males) participated, as listed in Table 1. This population is the same as that of our previous study,[16] which clarified CHD patients' spatial current abnormalities defined as a vessel-lesion diameter of >75%. The CHD patientswith two or three coronary-vessel lesions were defined as those with two lesions or three vessel lesions with diameters of ≥75%. We obtained informed consent from all participants and received approval from relevant ethical committees. Moreover, the CHD patients were classified into two groups, namely, ischemic (n = 12) or MI (n = 12), to evaluate the detection performance for ischemia, and patients with both ischemic and infarct areas were excluded. The ischemia and MI patients could be categorized as a minor part of the CHD patients because these patients were examined by SPECT.

MCG Recordings and Setup

MCG recording was performed above the chest of each participant for 30 seconds. The MCG signals were detected with a 64-channel MCG system (Hitachi High-Technologies Ltd., Tokyo, Japan)[17] in a magnetically shielded room. The detected MCG signals were passed through an analog band-pass filter (0.1–100 Hz) and an analog notch filter (50 Hz). The signals were then digitized at a sampling rate of 1 kHz by using an analog-digital converter. To remove the noise in the signals, the MCG data were averaged 20–30 times by using an ECG signal trigger. The MCG data were measured at three hospitals (Hitachi General Hospital, the National Cardiovascular Center, and University of Tsukuba Hospital) by using the same MCG system with the same sensitivity.

Table 1. Numbers of CHD and Control Patients

	N (n = 101)	CHD (n = 56)
Age (years)	63 ± 3	65 ± 6
Gender		
Female/Male	31 / 70	10 / 46
BMI	23.7	24.0
HR	63	63
SVD		25
LAD		16 (P:6, M: 5, D: 0, U: 5)
LCX		3 (P:1, M: 0, D: 1, U: 1)
RCA		6 (P:1, M: 2, D: 2, U: 1)
DVD		12
		LAD + LCX: 6
		LAD + RCA: 4
		LCX + RCA: 2
TVD		19

CHD = coronary heart disease, coronary artery lesion (> 75%); D = distal coronary artery; DVD = double vessel disease; LAD = left anterior descending coronary artery; LCX = left circumflex coronary artery; M = middle coronary artery; N = age-matched normal controls with no history of cardiovascular disease and normal electrocardiogram (ECG) at rest; P = proximal coronary artery; RCA = right coronary artery; SVD = single vessel disease; TVD = triple vessel disease; U = unknown precise location.

Production of Subtracted MCG Waveforms

We focused on the ST-T segment in the MCG waveforms because previous studies reported that electrical current abnormality in CHD patients appears during ventricular repolarization in MCGs.[7–15] The T end of each patient was manually defined by using overlapped MCG waveforms.[5]

A subtracted ST-T waveform was calculated by subtracting the standard MCG waveform, which was produced by averaging the 464 normal control patients' MCGs,[6] from the measured MCG waveforms on each channel. Figure 1 shows the procedure for subtracting the ST-T waveforms. The time

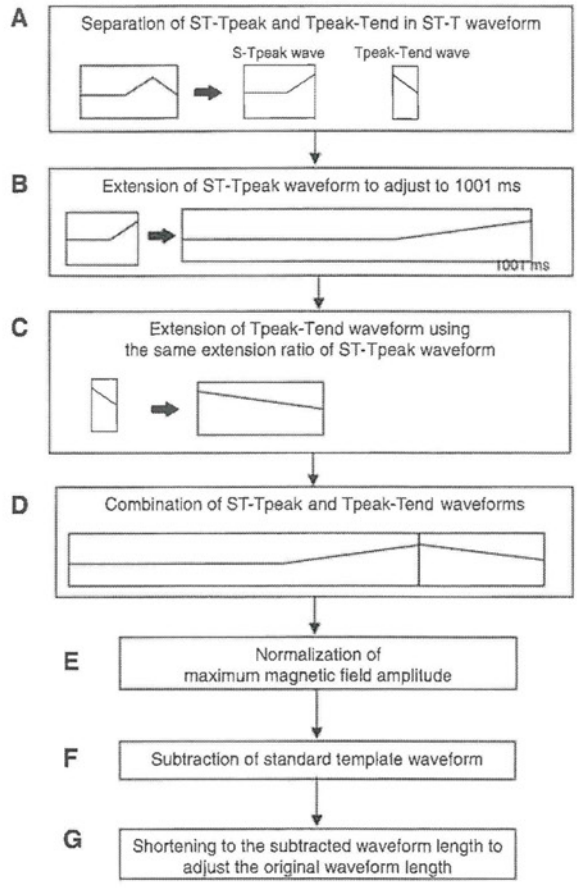

Figure 1. Procedure of subtracting ST-T waveform.

at which the amplitude of the ST-T waveform is a maximum varied among participants. The ST-T waveforms are, therefore, first separated into two parts, namely, an ST-Tpeak and a Tpeak-Tend, as shown in Figure 1A. Second, the ST-Tpeak waveforms are extended to 1001 milliseconds (Fig. 1B) by using the ratio of the duration of the ST-Tpeak waveform to the extended waveform. Third, the Tpeak-Tend waveforms are extended to 1001 milliseconds by using the same ratio for each participant (Fig. 1C).

In the next step, the ST-Tpeak and Tpeak-Tend waveforms are combined (Fig. 1D). The time interval of the data is lengthened by adding data points with zero amplitude after the Tend, and the amplitude of the magnetic field of both the Tpeak and Tpeak-Tend waveforms is normalized (Fig. 1E). The standard template waveform is then subtracted from the normalized ST-T waveforms (Fig. 1F). Finally, the time interval of the subtracted ST-T-waveforms is shortened to fit the original time interval (Fig. 1G). The subtracted ST-T MCG waveforms for each participant were obtained by this procedure.

Evaluation Method for Subtracting Waveforms

MCG parameters, which can be produced from the amplitude of the magnetic field and current distribution, are used to quantitatively evaluate the residual MCG signals in the subtracted ST-T waveforms. To investigate the current distribution, a current-arrow map (CAM) is used to indicate current vectors in the heart. The CAM indicates pseudo currents (Ix and Iy) defined by the derivatives of the normal component (Bz) of the MCG signals as

$$I_{x,n} = \frac{dB_{z,n}}{dy} \tag{1}$$

and

$$I_{y,n} = -\frac{dB_{z,n}}{dx}. \tag{2}$$

The magnitude of the current arrows ($I_{x,y} = \sqrt{(I_{x,n})^2 + (I_{y,n})^2}$) is plotted as a contour map, where n indicates channel number. The CAM helps in interpreting spatial heart electrical activity, and it can visualize the residual current component.

The above-mentioned CAM and the amplitude of the magnetic field at the Tpeak are used to calculate the following five parameters (three magnitude parameters and two two-dimensional distribution parameters).

1. Absolute value of the maximum amplitude of all MCG signals.
2. Absolute value of the maximum vector amplitude of all current vectors.
3. Maximum amplitude of total current vector (TCV).

The TCV[5,18] is obtained by summing all current arrows. The TCV ($\mathbf{I}$) of all current arrows can be calculated as a vector value by using the current arrow ($\mathbf{I_n}$) at each sensor,

$$\mathrm{I} = \sum_{n=1}^{64} \mathrm{I_n}(T), \tag{3}$$

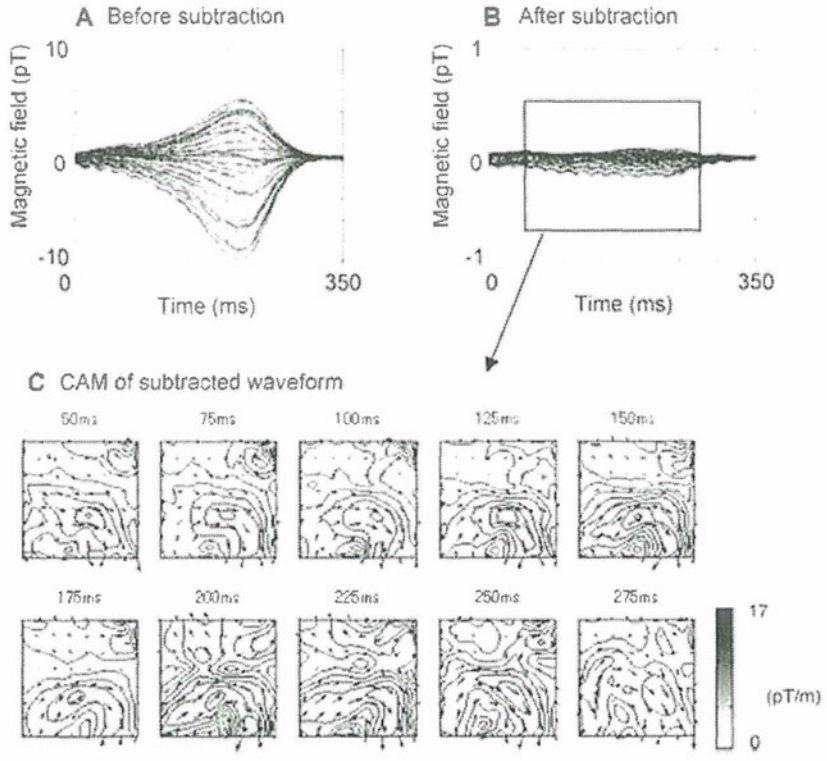

Figure 2. Subtracted ST-T waveform and current-arrow map (CAM) of typical normal control. (A) Original ST-T waveform. (B) Subtracted ST-T waveform. (C) CAM of (B).

where T is the calculated time. The TCV amplitude of the subtracted waveform is used because TCV has high sensitivity for detecting CHD.

4. Area ratio of abnormal current vector appearance.

Average (A) and standard deviation (σ) of the maximum current vector derived from step 2 in all healthy control patients were calculated in order to evaluate the abnormal current area. The number of current vectors with abnormal values above $A + \sigma$ is counted, and the number of abnormal current vectors is divided by total channel number, 64. The result of this division (given as a percentage) is used as the ratio of the areas where abnormal current vectors appear in the participant and control patients, hereafter referred to as the "area ratio of abnormal-current-vector appearance." For example, 100% indicates that all channels have abnormal values ($> A + \sigma$), and 25% indicates that 16 channels have abnormal values ($> A + \sigma$).

5. Two-dimensional frequency distribution of abnormal-current appearance

In the same manner as step 4, the number of appearances of abnormal-current vectors above $A + \sigma$ on each channel for each lesion group of CHD patients count is counted. The number (given as a percentage) is divided by the total number of participants in each lesion group. The number of appearances is plotted as a two-dimensional contour map of cumulative frequency. For instance, the 100% position in the two-dimensional contour map of three-vessel stenosis indicates that the 100% position always has an abnormal value ($> A + \sigma$). In this study, a two-dimensional contour map of each lesion group of the coronary artery was drawn.

RESULTS

Typical Subtracted ST-T waveform

A typical subtracted ST-T waveform and CAM of a healthy control is shown in Figure 2. While

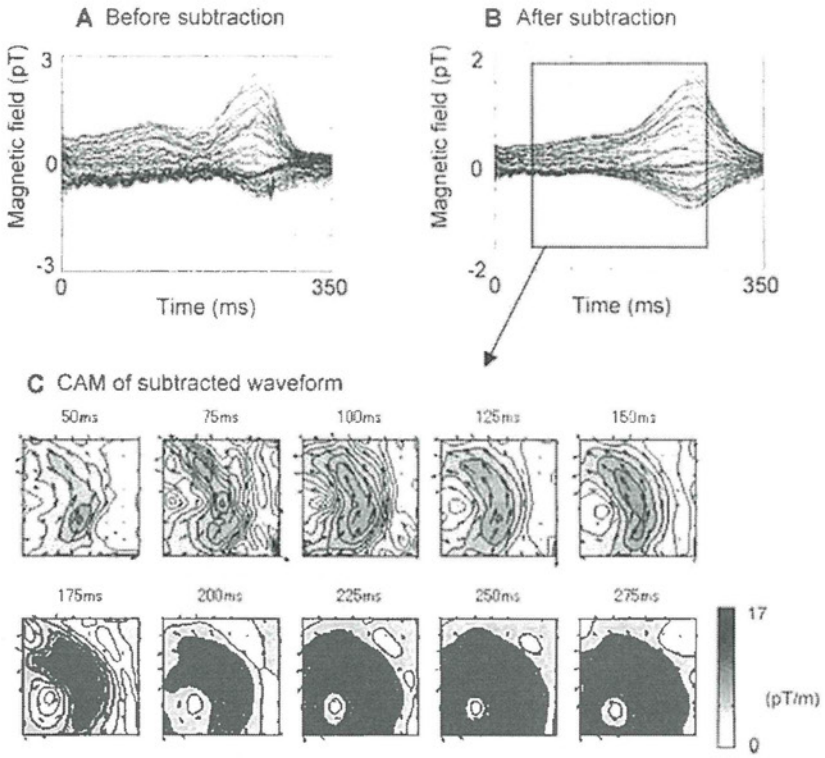

Figure 3. Subtracted ST-T waveform and current-arrow map (CAM) of typical CHD patient with triple vessel lesion. (A) Original ST-T waveform. (B) Subtracted ST-T waveform. (C) CAM of (B).

the amplitude of the ST-T waveform ranges from about −10 to 5 pT (Fig. 2A) before subtraction, the residual amplitude is very small (Fig. 2B) after subtraction, ranging from about −0.02 to 0.01 pT. In this case, up to 99.8% of the ST-T waveform can be removed. In the CAM in Figure 2C, the current vectors have small amplitude, and the residual currents are weaker than those before subtraction.

Figure 3 shows a typical subtracted ST-T waveform and the CAM of triple vessel disease (TVD) in CHD patients. The amplitude of the ST-T waveform ranges from about −1 to 2.5 pT (Fig. 3A) before the subtraction procedure, and the amplitude after the procedure is still high, ranging from about −0.9 to 1.8 pT. The reduction rate is about 23%. In the CAM in Figure 3C, a right upward current with high amplitude (about 24 pT/m) appears. This pattern, with large residual ST-T components, is found in almost all CHD patients.

Relationship between Parameters and Coronary-Artery Lesions

Figure 4 shows the maximum amplitude of the magnetic field, maximum current vector, maximum amplitude of the TCV, and area ratio of abnormal current vector appearance, which were calculated from the subtracted ST-T waveform and its CAM of the control and CHD patients. In the case of all parameters, the mean values increase with increasing number of coronary artery lesions. The difference between control and lesion parameters is significant ($P < 0.01$).

The sensitivity and specificity of the MCG for detecting CHD by using these four MCG parameters, listed in Table 2, were calculated. Criteria for each parameter are defined as the mean value plus the standard deviation for healthy control patients. In Table 2, the maximum amplitude of the TCV is highly sensitive (i.e., 74%) and has specificity of 84%, and the area ratio of abnormal current vector appearance has the highest specificity of 92.2%.